Palmitoylation-dependent association with CD63 targets the Ca^{2+} sensor synaptotagmin VII to lysosomes

Andrew R. Flannery,[1,2] Cecilia Czibener,[3] and Norma W. Andrews[1,2]

[1]Department of Cell Biology and Molecular Genetics, University of Maryland, College Park, MD 20742
[2]Section of Microbial Pathogenesis, Yale University School of Medicine, New Haven, CT 06510
[3]Instituto de Investigaciones Biotecnologicas, Instituto Tecnológico de Chascomús, Universidad Nacional de San Martín, Consejo Nacional de Investigaciones Científicas y Técnicas, 1650 Buenos Aires, Argentina

Syt VII is a Ca^{2+} sensor that regulates lysosome exocytosis and plasma membrane repair. Because it lacks motifs that mediate lysosomal targeting, it is unclear how Syt VII traffics to these organelles. In this paper, we show that mutations or inhibitors that abolish palmitoylation disrupt Syt VII targeting to lysosomes, causing its retention in the Golgi complex. In macrophages, Syt VII is translocated simultaneously with the lysosomal tetraspanin CD63 from tubular lysosomes to nascent phagosomes in a Ca^{2+}-dependent process that facilitates particle uptake. Mutations in Syt VII palmitoylation sites block trafficking of Syt VII, but not CD63, to lysosomes and phagosomes, whereas tyrosine replacement in the lysosomal targeting motif of CD63 causes both proteins to accumulate on the plasma membrane. Complexes of CD63 and Syt VII are detected only when Syt VII palmitoylation sites are intact. These findings identify palmitoylation-dependent association with the tetraspanin CD63 as the mechanism by which Syt VII is targeted to lysosomes.

Introduction

Synaptotagmins comprise a family of type I membrane proteins characterized by a short N-terminal region, a single transmembrane domain, a variable spacer region, and two highly conserved cytosolic C2 domains. Most synaptotagmins bind Ca^{2+} through their C2 domains, and the two most abundantly expressed isoforms, synaptotagmin I (Syt I) and synaptotagmin VII (Syt VII), were shown to directly confer Ca^{2+} sensitivity to membrane fusion reactions (Bhalla et al., 2005). Syt I expression is largely restricted to neurons (Li et al., 1995), where it regulates Ca^{2+}-triggered exocytosis of synaptic vesicles and neurotransmitter release (Chapman, 2008). Syt VII is more broadly expressed (Li et al., 1995), being localized on secretory granules of pancreatic cells (Gao et al., 2000; Gauthier et al., 2008; Gustavsson et al., 2009) and on lysosomal compartments of several cell types, from fibroblasts and epithelial cells to macrophages and dendritic cells (Martinez et al., 2000; Fukuda et al., 2004; Czibener et al., 2006; Monterrat et al., 2007; Zhao et al., 2008; Becker et al., 2009).

Functional inhibition or genetic ablation experiments showed that Syt VII regulates Ca^{2+}-dependent insulin and glucagon secretion by pancreatic cells (Li et al., 2007; Gauthier et al., 2008; Gustavsson et al., 2008, 2009) and the exocytosis of conventional lysosomes in several cell types (Martinez et al., 2000; Andrews and Chakrabarti, 2005; Czibener et al., 2006). Ca^{2+}-triggered lysosomal exocytosis is a major component of the process by which eukaryotic cells repair lesions on their plasma membrane (Reddy et al., 2001; Keefe et al., 2005; Idone et al., 2008). Ca^{2+}-regulated delivery of lysosomal membranes to the cell surface is also involved in the phagocytic uptake of particles by macrophages (Braun et al., 2004; Czibener et al., 2006). Mutations in the Ca^{2+}-binding residues of the C2 domains inhibit Syt VII mobilization to nascent phagosomes and abolish a Ca^{2+}-dependent component of the phagocytic process (Czibener et al., 2006). These findings led to the hypothesis that Syt VII–containing microdomains might have unique properties that favor their rapid

Correspondence to Norma W. Andrews : andrewsn@umd.edu

Abbreviations used in this paper: 2-BP, 2-bromopalmitate; BMM, bone marrow macrophage; CMV, cytomegalovirus; GalT, galactosyltransferase 1; NRK, normal rat kidney; TEM, tetraspanin-enriched microdomain.

The Rockefeller University Press $30.00
J. Cell Biol. Vol. 191 No. 3 599–613
www.jcb.org/cgi/doi/10.1083/jcb.201003021

mobilization to the cell surface during Ca^{2+}-triggered phagocytosis and plasma membrane repair.

Despite the limited amount of unique sequence information within the synaptotagmin family, different isoforms are sorted to distinct subcellular sites. There is still very little information about the mechanisms responsible for this differential intracellular targeting. Trafficking of the neuronal isoform Syt I to synaptic vesicles (Matthew et al., 1981; Kabayama et al., 1999) was attributed to a dihydrophobic methionine-leucine motif within its extreme C terminus (Blagoveshchenskaya et al., 1999), although posttranslational modifications at the N terminus such as N-glycosylation (Han et al., 2004), O-glycosylation (Fukuda, 2002; Kanno and Fukuda, 2008), and palmitoylation (Heindel et al., 2003; Kang et al., 2004) were also proposed to play a role. The trafficking of Syt II (Geppert et al., 1991) to neurite terminals was also linked to a C-terminal two-residue motif (Krasnov and Enikolopov, 2000), whereas a unique region within the spacer domain of Syt IV was found to be necessary for Golgi targeting in PC-12 cells (Fukuda et al., 2001a). Syt IX, an isoform reported to control the exocytosis of β-cell granules (Iezzi et al., 2004) and dense core vesicles in PC-12 cells (Fukuda et al., 2004), is sorted to recycling endosomes in RBL-2H3 and CHO cell lines by a mechanism dependent on PKC-mediated phosphorylation (Haberman et al., 2005).

Given the absence of classical lysosomal targeting motifs (Braulke and Bonifacino, 2009) in the Syt VII sequence, the steady-state localization of this isoform on lysosomes has been particularly puzzling. An insight into this issue was provided by the detection of Syt VII on discrete microdomains of lysosomal compartments in macrophages, which are rapidly translocated to the cell surface at sites of phagocytosis (Czibener et al., 2006). These findings led us to investigate a possible role for dynamic tetraspanin-enriched microdomains (TEMs) in the intracellular trafficking of Syt VII. Our results demonstrate that palmitoylation-dependent association with the lysosomal tetraspanin CD63 is a requirement for the intracellular trafficking of Syt VII from the Golgi complex to lysosomes.

Results

Syt VII palmitoylation sites are required for lysosomal targeting and efficient phagocytosis in macrophages

Cysteine residues located close to the boundary between transmembrane and cytoplasmic regions were identified as serine palmitoylation sites in numerous membrane proteins (for review see Charollais and Van Der Goot, 2009). With the exception of Syt XII, all the 17 known synaptotagmin isoforms contain at least one cysteine in this region (Heindel et al., 2003; Prescott et al., 2009). Syt VII has three cysteines within and adjacent to the transmembrane domain, C35, C38, and C41 (Fig. 1 A). Earlier work showed that replacement of these three cysteines by alanine abolishes Syt VII palmitoylation, which was determined by [^{3}H]palmitate incorporation assays (Kang et al., 2004). Because mutations in individual cysteines can result in alternative acylation of neighboring cysteines (Abrami et al., 2006), to assess the role of palmitoylation in Syt VII localization, we first generated a fluorescently tagged construct in which all the three putative palmitoylation sites were replaced by serines (Syt VII (C/S)–YFP).

An earlier study showed that bone marrow macrophages (BMMs) from Syt VII–deficient mice (Syt VII$^{-/-}$) are impaired in the phagocytosis of large particles (Czibener et al., 2006). Phagocytosis was restored to control levels by expression of wild-type Syt VII–YFP, but a Syt VII (D/N)–YFP construct carrying mutations in the Ca^{2+}-binding sites did not rescue the phenotype (Czibener et al., 2006). We further investigated this role of Syt VII in phagocytosis by examining the effect of mutations in the Syt VII palmitoylation sites. Adenoviral-mediated expression of the mutated Syt VII (C/S)–YFP construct in Syt VII$^{-/-}$ BMMs did not restore the phagocytosis of zymosan particles to the same levels observed after expression of wild-type Syt VII–YFP (Fig. 1 B). The lack of complementation of the phagocytosis phenotype was not caused by lower expression levels because similar amounts of Syt VII–YFP, Syt VII (D/N)–YFP, and Syt VII (C/S)–YFP were detected in the transduced BMMs (Fig. 1 C). Imaging experiments revealed a markedly altered localization of the palmitoylation-defective Syt VII (C/S)–YFP construct in BMMs. Although Syt VII–YFP, as expected, was targeted to Lamp1-positive tubular lysosomal compartments (Czibener et al., 2006), Syt VII (C/S)–YFP did not colocalize with Lamp1, being detected in centrally located globular compartments (Fig. 1 D). These results indicate that palmitoylation is required for Syt VII to reach lysosomes and to participate in the phagocytic process.

Syt VII palmitoylation sites are required for Syt VII delivery to nascent phagosomes, simultaneously with the lysosomal tetraspanin CD63

Three-color live spinning-disk confocal microscopy was used to follow the distribution of the Syt VII–YFP or Syt VII (C/S)–YFP in relation to two lysosomal proteins, Lamp1-RFP and CFP-CD63, during the uptake of zymosan particles by Syt VII$^{-/-}$ BMMs. Whereas Syt VII–YFP and the two other lysosomal proteins colocalized in BMM lysosomal compartments, only Syt VII–YFP and CFP-CD63 were rapidly translocated to nascent phagosomes. Lamp1-RFP, as previously shown (Czibener et al., 2006), was delivered to phagosomes with a delayed kinetics after the initial extension of Lamp1-positive tubules around newly formed phagosomes (Fig. 2 A and Video 1). In contrast, Syt VII (C/S)–YFP accumulated in a perinuclear compartment that did not contain lysosomal markers and was not targeted along with CFP-CD63 to nascent phagosomes. The tubular extensions containing Lamp1-RFP observed around recent phagosomes also appeared to be less abundant in BMMs expressing Syt VII (C/S)–YFP, although Lamp1 was detected on phagosomes at later time points (Fig. 2 B and Video 2). These observations demonstrate that the lysosomal membrane proteins Syt VII and CD63 traffic rapidly and simultaneously to phagosomes, but in the absence of palmitoylation, Syt VII fails to reach lysosomes and to be delivered along with CD63 to nascent phagosomes.

Syt VII is retained in the Golgi apparatus in the absence of palmitoylation

To facilitate characterization of the perinuclear compartment where the palmitoylation-defective Syt VII (C/S)–YFP accumulated,

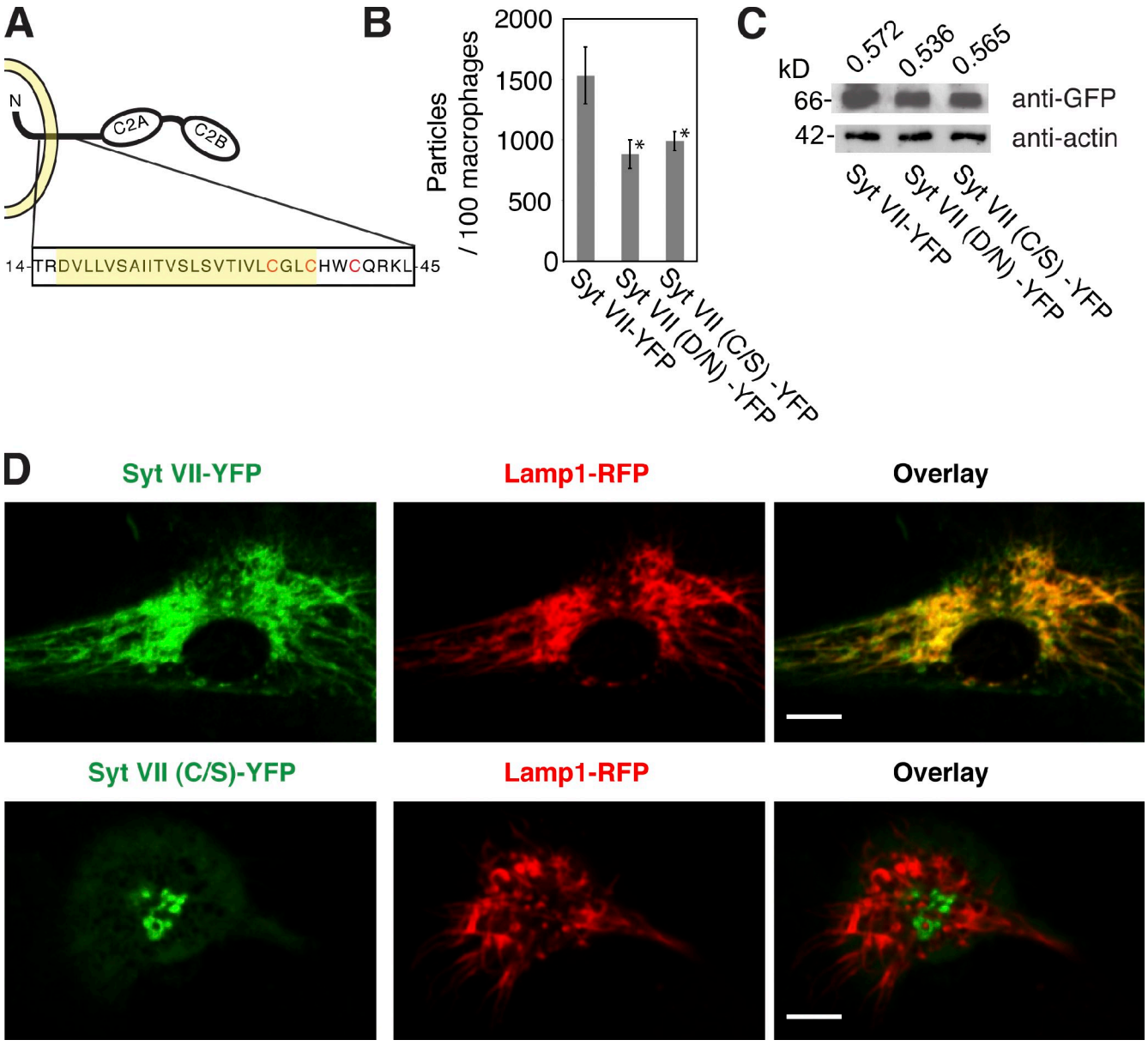

Figure 1. **Mutations in Syt VII palmitoylation sites cause defects in lysosomal targeting and BMM phagocytosis.** (A) Schematic model of Syt VII depicting in red the three cysteines (C35, C38, and C41) adjacent to the transmembrane domain (highlighted in yellow) that were mutated to serines in Syt VII (C/S)–YFP. (B) Phagocytosis levels were quantified in Syt VII$^{-/-}$ BMMs transduced with adenovirus expressing Syt VII–YFP, Syt VII (D/N)–YFP, and Syt VII (C/S)–YFP after exposure to 25 zymosan particles per cell for 1 h. The reduced phagocytosis that is observed in Syt VII$^{-/-}$ BMMs was rescued by wild-type Syt VII–YFP, but not by Syt VII (D/N)–YFP (the Ca^{2+}-binding mutant) or Syt VII (C/S)–YFP (the palmitoylation mutant). The asterisk indicates statistically significant differences from the control construct Syt VII–YFP (Student's *t* test, $P < 0.05$). The data represent the means, and the error bars represent the standard deviation of triplicate determinations. (C) Western blot of the transduced Syt VII$^{-/-}$ BMM cell lysates with anti-GFP antibodies showing comparable amounts of expressed Syt VII–YFP, Syt VII (D/N)–YFP, or Syt VII (C/S)–YFP. The bottom panel shows the loading control, which was probed with antiactin antibodies. The values on top reflect the ratio of Syt VII/actin quantified by ImageJ software. (D) Live confocal images of Syt VII$^{-/-}$ BMMs transduced with adenovirus encoding Syt VII–YFP or Syt VII (C/S)–YFP and Lamp1-RFP. Syt VII–YFP colocalizes with Lamp1 on tubular lysosomes, but Syt VII (C/S)–YFP does not. Bars, 6 µm.

we performed colocalization experiments in normal rat kidney (NRK) cells. Unlike in BMMs where the lysosomal compartment is extensively tubulated, in NRK cells, lysosomes appear as well-defined vesicular compartments. In agreement with earlier studies (Martinez et al., 2000; Caler et al., 2001; Jaiswal et al., 2002), Syt VII–YFP colocalized with Lamp1-RFP in live NRK cells, whereas Syt VII (C/S)–YFP was mistargeted to a perinuclear compartment resembling Golgi cisternae (Fig. 3 A). The palmitoylation-deficient Syt VII construct and the Golgi enzyme galactosyltransferase 1 (GalT; Schaub et al., 2006) fused to RFP (GalT-RFP) fully colocalized when coexpressed in NRK cells (Fig. 3 B), confirming a Golgi localization of the palmitoylation-defective Syt VII. The same was observed in transduced BMMs (Fig. S1). Colocalization was also observed in NRK cells between Syt VII (C/S)–YFP and antibodies to endogenous TGN38, a TGN marker (Fig. 3 C).

The effect of individually mutating each of the three cysteines adjacent to the transmembrane domain was also investigated.

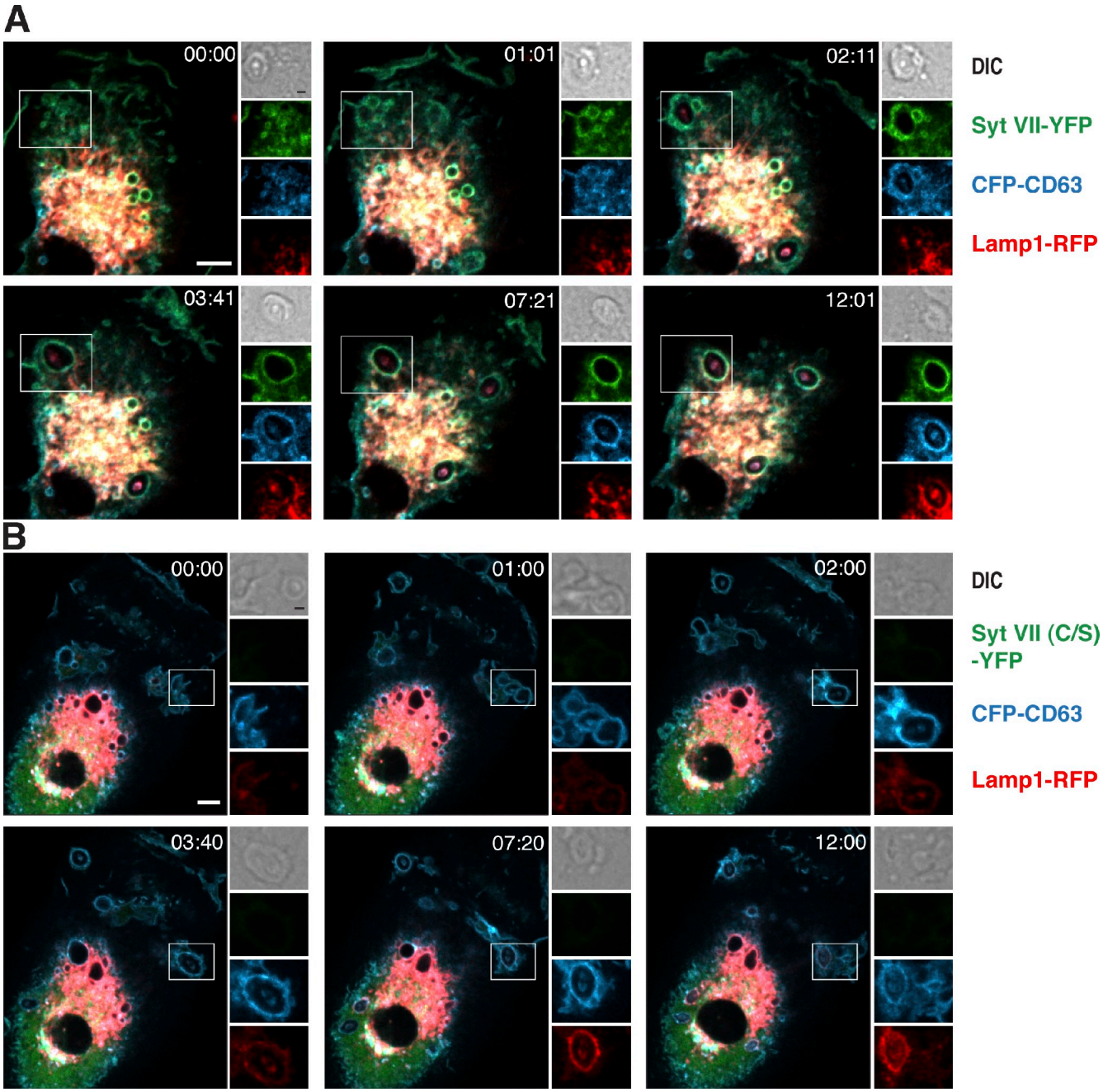

Figure 2. **Time-lapse imaging of the recruitment of Syt VII, Syt VII (C/S), CD63, and Lamp1 to nascent phagosomes.** Syt VII$^{-/-}$ BMMs transduced with adenovirus expressing CFP-CD63, Lamp1-RFP, and Syt VII–YFP or Syt VII (C/S)–YFP were exposed to 10 zymosan particles per cell and imaged by live confocal time-lapse microscopy. (A) Selected video frames showing that Syt VII–YFP and CFP-CD63 are simultaneously recruited to nascent phagosomes, followed by membrane tubules containing Lamp1-RFP (Video 1). (B) Selected video frames showing that CFP-CD63 is recruited to nascent phagosomes, but Syt VII (C/S)–YFP is not (Video 2). The differential interference contrast (DIC)–, YFP-, CFP-, and RFP-dissociated images for each highlighted phagosome (inset boxes) are shown on the right. Bars, 6 µm.

The C35S, C38S, or C41S Syt VII–YFP constructs behaved similarly, being partially retained in the perinuclear area (Fig. 4). When pairs of cysteines were mutated (C35/41S, C35/38S, or C38/41S), full retention in the Golgi was observed, similar to what occurs when all three cysteines are replaced (Syt VII (C/S)–YFP; Fig. 4). These results strongly suggest that C35, C38, and C41 can all be palmitoylated and contribute in a dose-dependent manner to the trafficking of Syt VII out of the Golgi and into lysosomes.

Consistent with the mutagenesis results, treatment of NRK cells with the potent palmitoylation inhibitor 2-bromopalmitate (2-BP) also caused Golgi retention of Syt VII–YFP (Fig. 5, A and B) without further disrupting the mislocalization of Syt VII (C/S)–YFP (Fig. 5 C). Although CD63 is also palmitoylated (Yang et al., 2002), 2-BP treatment did not affect its colocalization with Lamp1 on lysosomes (Fig. 5 D). The retention of Syt VII–YFP in the Golgi induced by 2-BP was reversible, with full colocalization with Lamp1-RFP being

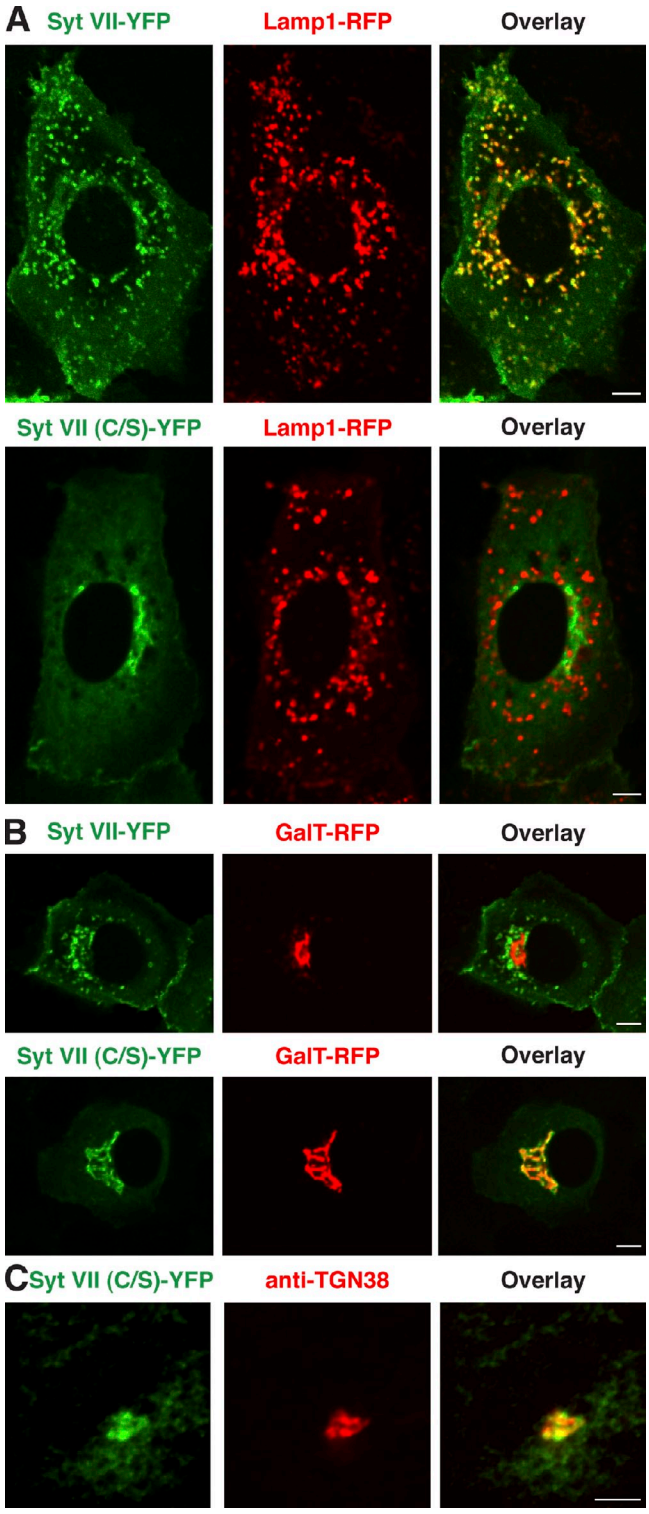

Figure 3. **Palmitoylation-site mutations lead to Syt VII retention in the TGN.** (A) NRK cells were transduced with adenovirus expressing Lamp1-RFP and Syt VII–YFP or Syt VII (C/S)–YFP and imaged by live confocal microscopy. Syt VII–YFP colocalizes with the lysosomal marker Lamp1-RFP, but Syt VII (C/S)–YFP does not. (B) NRK cells were transduced with adenovirus expressing GalT-RFP and Syt VII–YFP or Syt VII (C/S)–YFP and imaged by live confocal microscopy. Syt VII (C/S)–YFP colocalizes with the Golgi marker GalT-RFP, whereas Syt VII–YFP does not. (C) NRK cells were transduced with adenovirus expressing Syt VII (C/S)–YFP, fixed, labeled with antibodies to TGN38, and imaged by confocal microscopy. Syt VII (C/S) colocalizes with the trans-Golgi marker TGN38. Bars, 6 µm.

observed 24 h after washing out the inhibitor (Fig. 6 A). Live spinning-disk confocal microscopy detected vesicles containing Syt VII–YFP leaving the Golgi region and merging with Lamp1-RFP–positive lysosomes shortly after 2-BP removal from the culture medium (Fig. 6 B and Video 3). Thus, mutations or drugs that abolish palmitoylation disrupt Syt VII trafficking to lysosomes, resulting in its accumulation in the Golgi.

Syt VII is targeted to lysosomes through formation of a palmitoylation-dependent complex with the lysosomal tetraspanin CD63

Time-lapse live imaging of phagocytosis in BMMs revealed that Syt VII and CD63 are rapidly and simultaneously mobilized to the membrane of nascent phagosomes, whereas Lamp1 is delivered with slower kinetics (Fig. 2 A and Video 1). Together with earlier evidence that Syt VII forms microdomains on lysosomes that fully colocalize with CD63, but only partially with Lamp1 (Czibener et al., 2006), these observations suggested that the tetraspanin CD63 might play a role in the intracellular transport of Syt VII. We investigated this possibility by coexpressing Syt VII–YFP with CFP-CD63 carrying or not carrying a mutation in the critical tyrosine residue of its lysosomal targeting motif (Rous et al., 2002). As previously described (Rous et al., 2002), CFP-CD63 (Y/A) accumulated in the plasma membrane instead of trafficking to lysosomes. Importantly, when Syt VII–YFP was coexpressed with CFP-CD63 (Y/A), it was largely detected on the plasma membrane instead of lysosomes (Fig. 7 A). These results directly demonstrate that the lysosomal targeting motif of CD63 can direct the trafficking of Syt VII to lysosomes. The small fraction of Syt VII that reached lysosomes in cells expressing CFP-CD63 (Y/A) is likely to be a consequence of the presence of low levels of endogenous wild-type CD63 in NRK cells (Video 4).

Evidence has been accumulating that members of the tetraspanin family, which include CD63, engage in abundant lateral associations with each other and with other membrane-associated molecules, forming functional platforms known as tetraspanin "webs" or TEMs (Yang et al., 2002, 2004). The fact that trafficking of Syt VII to lysosomes depends on sorting signals present on CD63 suggests that these molecules interact as part of a palmitoylation-dependent TEM (Fig. 8). To investigate this possibility, we lysed cells expressing tagged constructs of both proteins under the low stringency detergent lysis conditions that are known to preserve TEM (Yang et al., 2002). We found that Syt VII–YFP and FLAG-CD63 are coimmunoprecipitated from 1% Brij-97 extracts when Syt VII palmitoylation sites are intact (Syt VII–YFP) but not when those sites are mutated (Syt VII (C/S)–YFP; Fig. 7 B). The FLAG-CD63 (Y/A) mutant that is incapable of trafficking to the lysosome was also coimmunoprecipitated with Syt VII–YFP, but not with Syt VII (C/S)–YFP (Fig. 7 C). Thus, the palmitoylation-dependent association of Syt VII with CD63, which is required for Golgi exit and lysosomal targeting, has the properties expected of a TEM. Mutation of the lysosomal

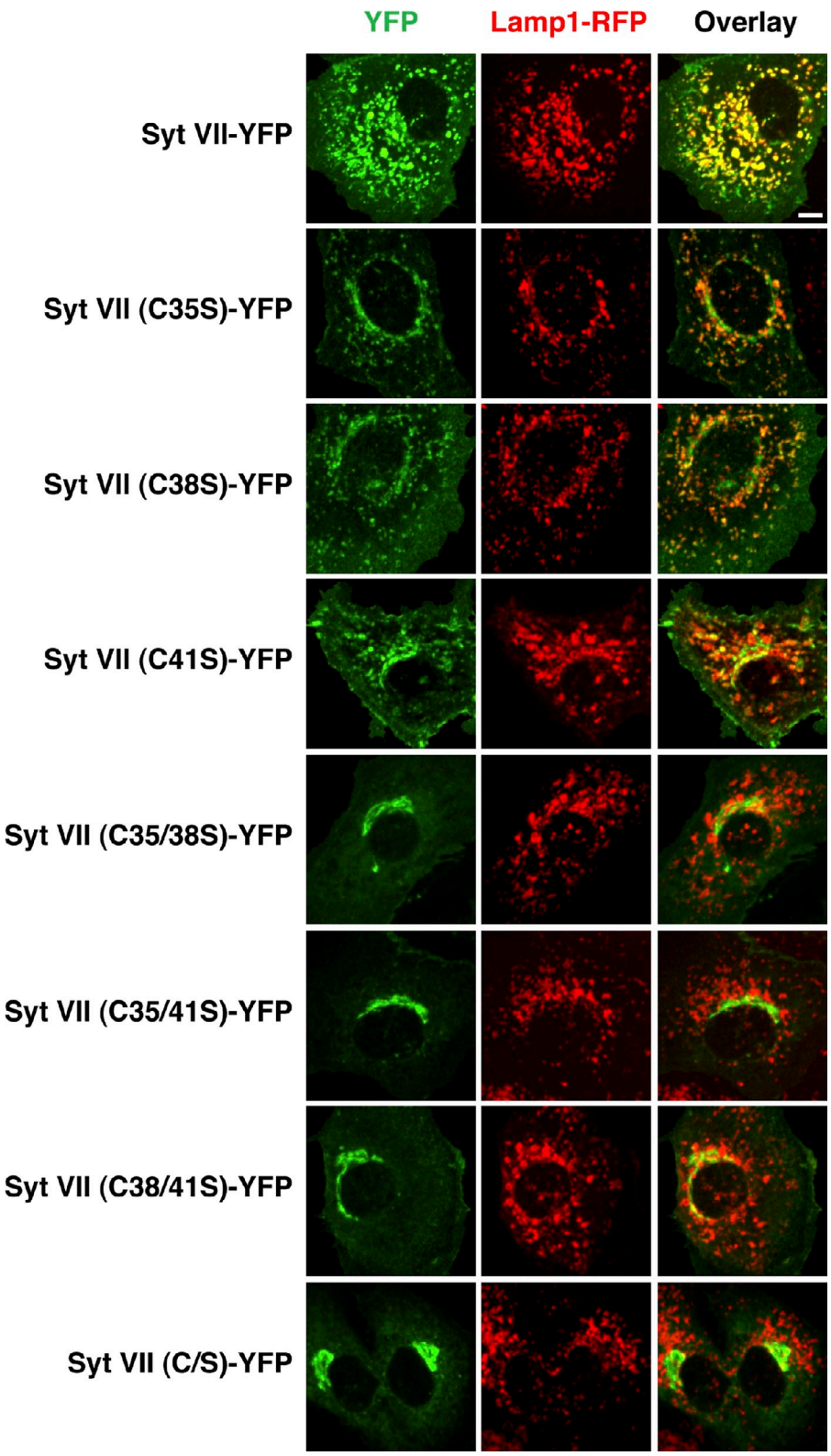

Figure 4. **The Syt VII membrane proximal cysteines C35, C38, and C41 are required for complete lysosomal localization.** NRK cells transduced with adenovirus expressing Lamp1-RFP and either Syt VII–YFP, Syt VII (C35S)–YFP, Syt VII (C38S)–YFP, Syt VII (C41S)–YFP, Syt VII (C35/38S)–YFP, Syt VII (C35/41S)–YFP, Syt VII (C38/41S)–YFP, or Syt VII (C/S)–YFP (green) were imaged by live confocal microscopy. Images represent maximum-intensity projections of 16 Z sections. Cells expressing Syt VII single-cysteine mutants display partial Syt VII localization to lysosomes and Golgi, whereas cells expressing Syt VII double- and triple-cysteine mutants display complete Golgi retention of Syt VII. Bar, 6 µm.

targeting motif of CD63 does not disrupt its TEM-like association with palmitoylated Syt VII, consistent with the ability of CD63 (Y/A) to cause mislocalization of wild-type Syt VII to the plasma membrane (Fig. 7 A).

siRNA-mediated silencing confirmed that CD63 is required for the exit of Syt VII from the TGN and targeting to lysosomes. When expressed in siRNA-treated HeLa cells, which showed a marked down-regulation of CD63 expression (Fig. 9, A and B), Syt VII–YFP was not able to reach lysosomes (Fig. 9 C, Lamp1-RFP) and was retained in the Golgi (Fig. 9 D, GalT-RFP). In contrast, a construct containing silent mutations that render the transcript resistant to silencing by

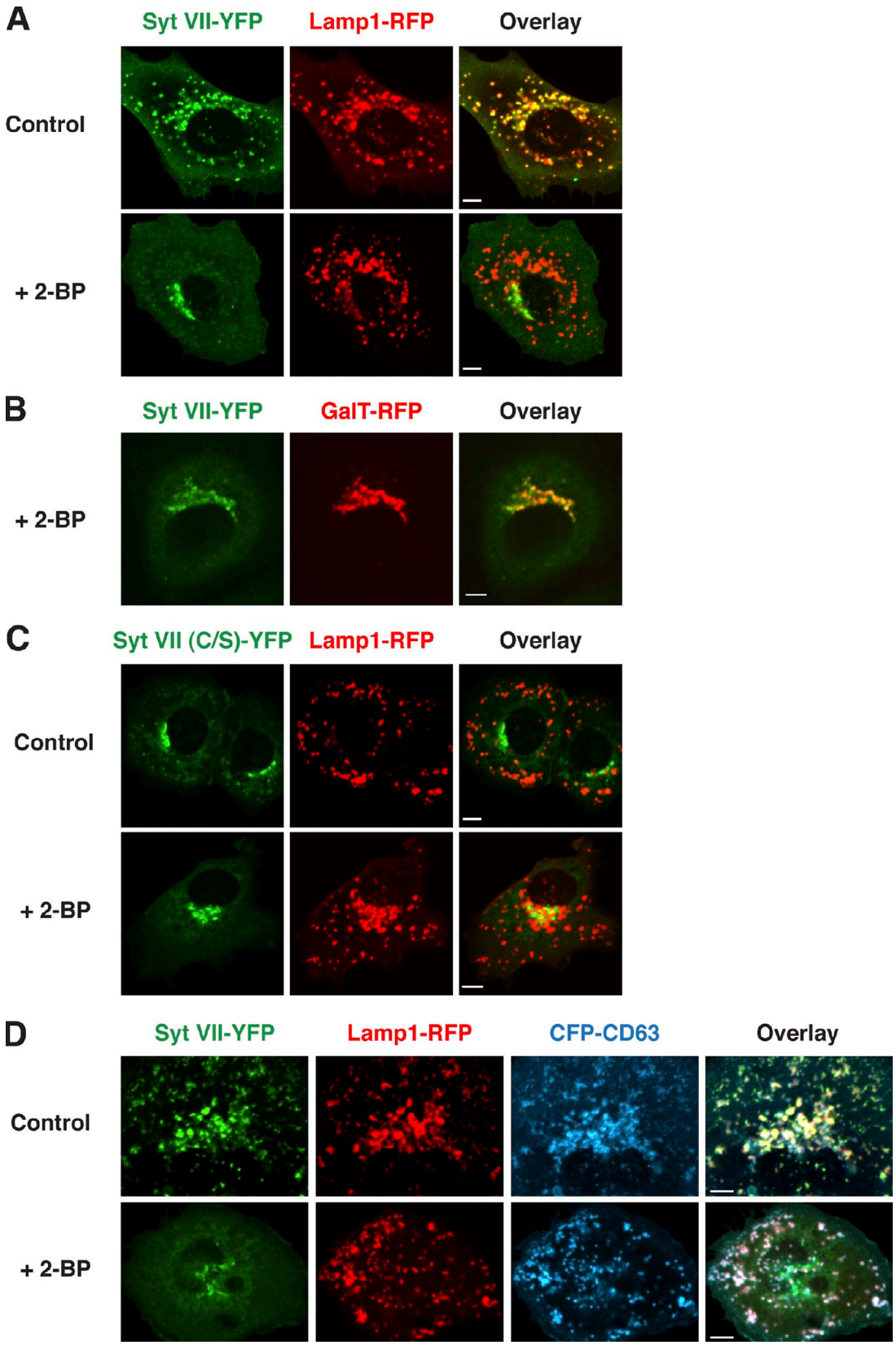

Figure 5. **Treatment with the palmitoylation inhibitor 2-bromopalmitate (2-BP) results in Syt VII–YFP retention in the TGN.** NRK cells transduced with adenovirus expressing Lamp1-RFP (A, C, and D), GalT-RFP (B), Syt VII–YFP (A, B, and D), Syt VII (C/S)–YFP (C), or CFP-CD63 (D) were imaged by live confocal microscopy after being treated with 100 μM 2-BP or carrier (Control) for 15 h. (A) Syt VII–YFP is mistargeted to globular structures resembling the Golgi apparatus in 2-BP–treated cells. (B) The globular structures containing Syt VII–YFP in 2-BP–treated cells colocalize with the trans-Golgi marker GalT-RFP. (C) The localization of Syt VII (C/S)–YFP does not change upon treatment with 2-BP. (D) The localization of CFP-CD63 on lysosomes is not altered by 2-BP treatment. Bars, 6 μm.

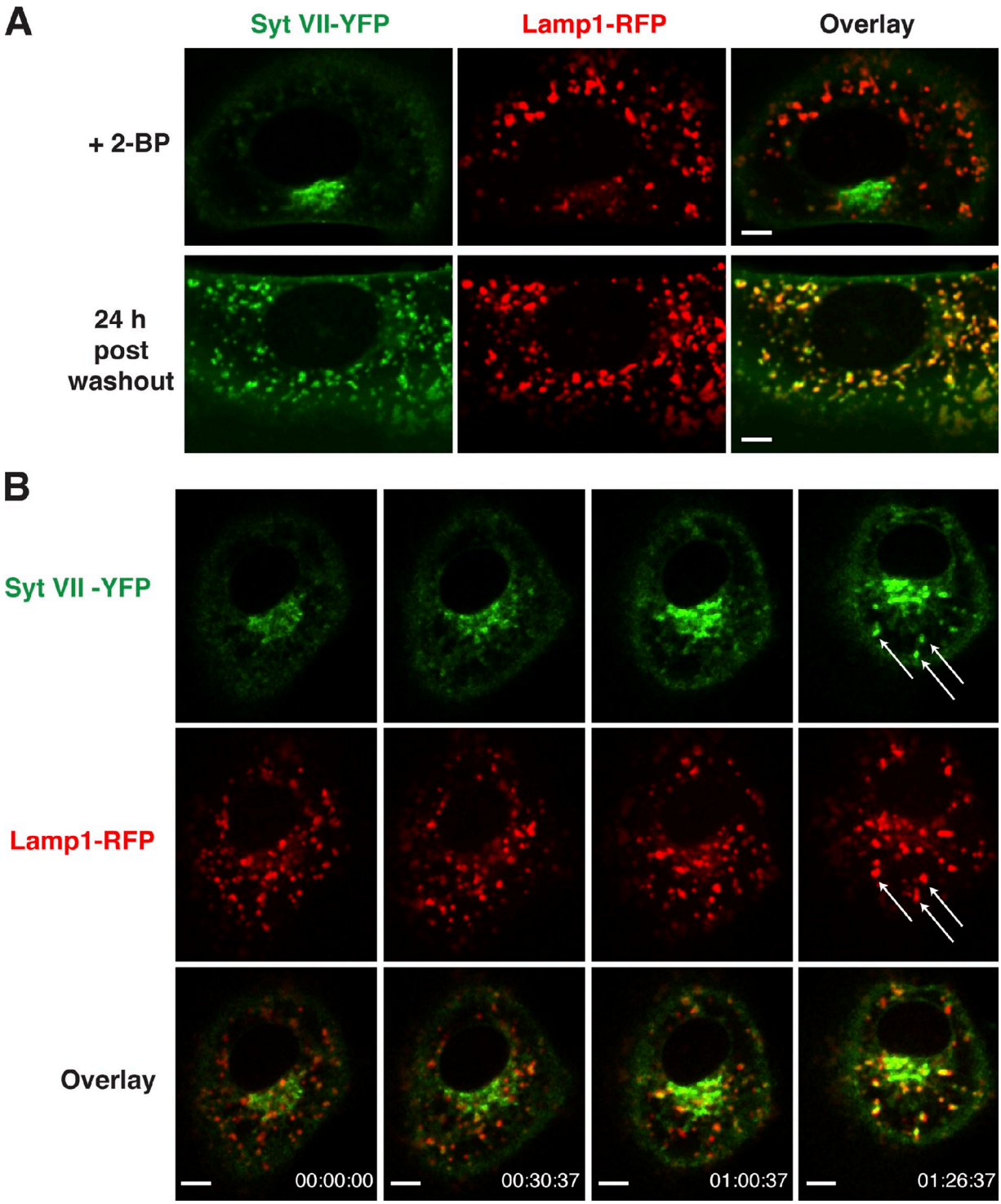

Figure 6. **Syt VII–YFP is targeted to Lamp1-positive compartments upon washout of 2-bromopalmitate (2-BP).** NRK cells were transduced with adenovirus expressing Syt VII–YFP and Lamp1-RFP, treated with 2-BP for 15 h, and imaged by live confocal microscopy. (A) Syt VII–YFP is detected in the Golgi in 2-BP–treated cells (top) but fully colocalizes with the lysosomal marker Lamp1-RFP 24 h after washout (bottom). (B) Selected frames of a live-imaging video acquired at the rate of 1 frame per minute for 86 min, immediately after 2-BP washout. Arrows indicate vesicles containing Lamp1-RFP that acquire Syt VII–YFP over time (Video 3). Bars, 6 µm.

the CD63 siRNA (CFP-resCD63) was targeted normally to Lamp1-containing lysosomes and did not cause Syt VII mislocalization (Fig. 9 E). Thus, Syt VII trafficking out of the TGN and into lysosomes specifically requires expression of the tetraspanin CD63.

Discussion

In this study, we characterize the mechanism by which Syt VII, a ubiquitously expressed member of the synaptotagmin family of Ca^{2+} sensors, is targeted to lysosomes in mammalian cells.

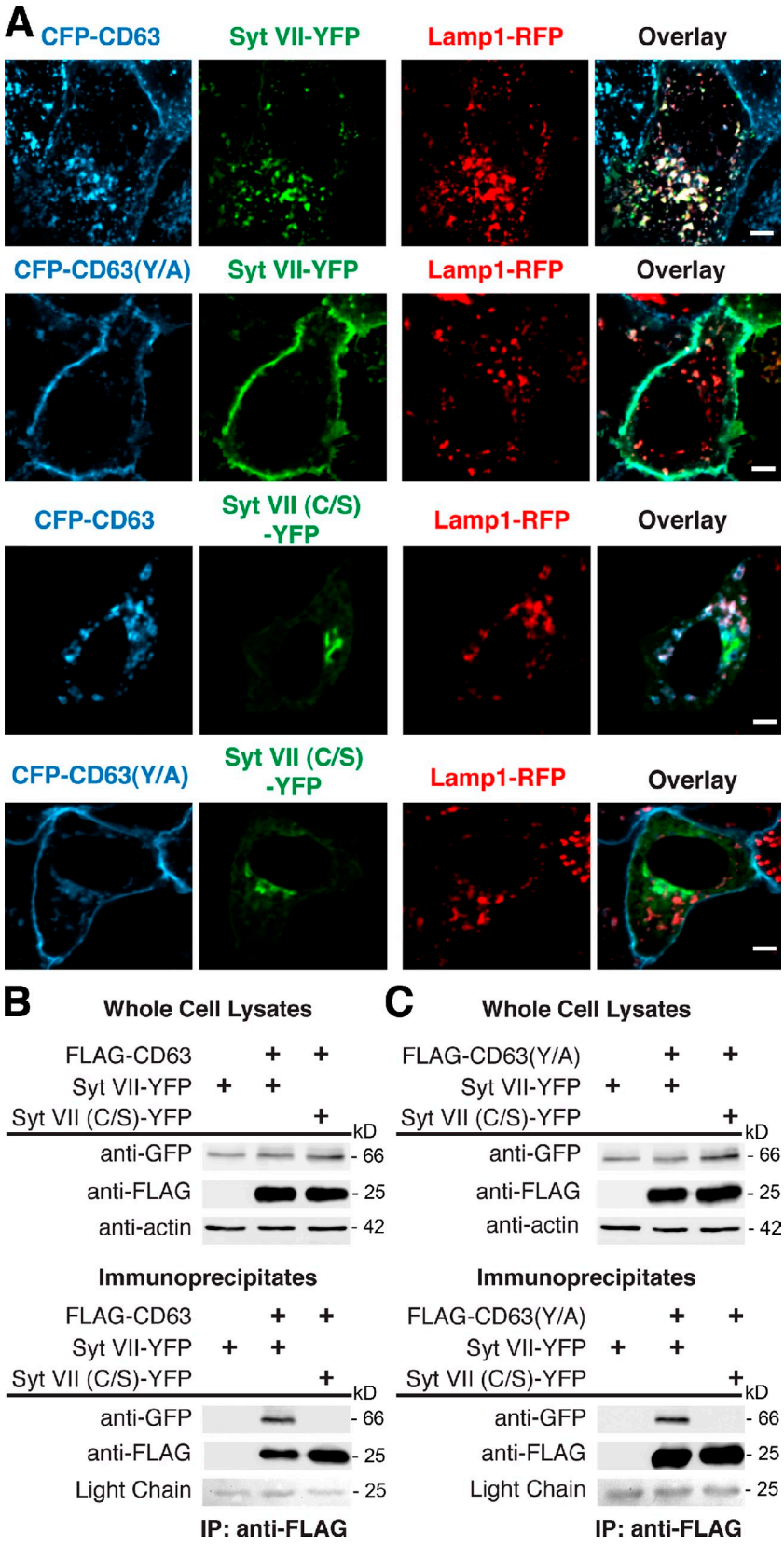

Figure 7. **Palmitoylation-dependent association with CD63 determines the localization of Syt VII.** (A) Mistargeting of CD63 affects the localization of Syt VII. NRK cells were transduced with adenovirus expressing Lamp1-RFP, Syt VII–YFP or Syt VII (C/S)–YFP, and CFP-CD63 or CFP-CD63 (Y/A) and imaged by live confocal microscopy. Syt VII–YFP and CFP-CD63 colocalize with Lamp1-RFP (top). CFP-CD63 (Y/A) lacking a functional lysosomal targeting motif localizes to the plasma membrane together with Syt VII–YFP (middle) but not with Syt VII (C/S), which is detected in the Golgi (bottom; Video 4) and (Video 5). Bars, 6 µm. (B and C) Syt VII coimmunoprecipitates with CD63 or CD63 (Y/A) only when palmitoylation sites are intact. NRK cells were transduced with adenovirus expressing FLAG-CD63 (B) or FLAG-CD63 (Y/A) (C) and Syt VII–YFP or Syt VII (C/S)–YFP, lysed in 1% Brij-97, and immunoprecipitated with anti-FLAG antibodies. The lysates and immunoprecipitates were subjected to immunoblot analysis with anti-GFP, anti-FLAG, or anti-actin antibodies. Ponceau S staining of the immunoglobulin light chain was used as a loading control in the immunoprecipitates. Coimmunoprecipitation was observed between FLAG-CD63 or FLAG-CD63 (Y/A) and Syt VII–YFP, but not with the palmitoylation-defective Syt VII (C/S)–YFP.

Our results show that Syt VII leaves the TGN and reaches lysosomes as part of a complex with the tetraspanin CD63. The GYEVM cytosolic motif that directs CD63 to lysosomes is known to be important for its association with the adaptor molecules AP-3 and AP-2, which mediate lysosomal targeting by both direct (TGN to lysosomes) and indirect (via the plasma membrane) routes, as well as retrieval from the plasma membrane by clathrin-dependent endocytosis (Rous et al., 2002; Bonifacino and

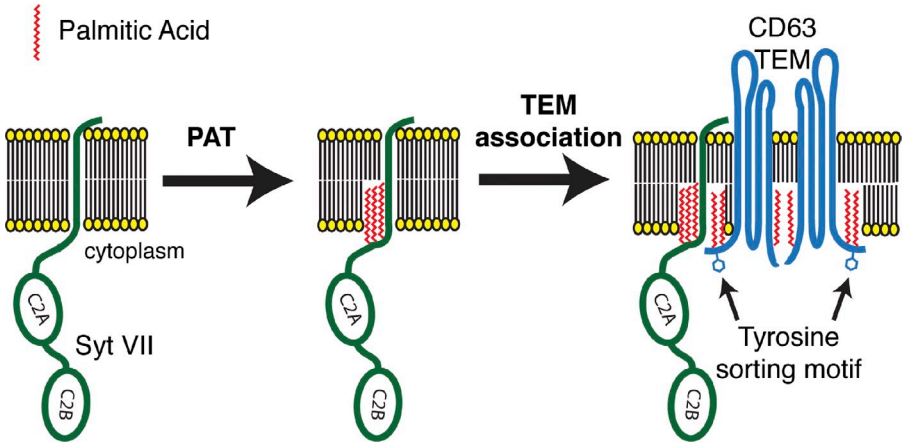

Figure 8. **Model of CD63-mediated trafficking of Syt VII.** Upon acylation by a Golgi-resident palmitoyl acyltransferase (PAT), Syt VII associates with CD63 within a TEM, being targeted to lysosomes through the lysosomal trafficking motif of CD63.

Traub, 2003). We found that replacement of the critical tyrosine residue in the GYEVM motif by alanine caused the expected accumulation of CD63 on the plasma membrane (Rous et al., 2002) and an identical mistargeting pattern for Syt VII. Furthermore, we found that CD63 expression is required for the trafficking of Syt VII out of the TGN and that palmitoylation of Syt VII is essential for its association with CD63.

Interactions with CD63 were previously shown to influence the intracellular trafficking of some membrane proteins, but most examples reported involve regulation of the internalization of plasma membrane–resident proteins (Skubitz et al., 2000; Duffield et al., 2003; Codina et al., 2005) or targeting for lysosomal degradation (Takino et al., 2003; Yoshida et al., 2008). Our present results indicate that association with CD63 is required for the exit of Syt VII from the TGN and its subsequent steady-state localization on lysosomes. Interestingly, there is evidence that CD63 participates in the transport of neutrophil elastase to secretory granules (Källquist et al., 2008), indicating that this pathway may also be important for the trafficking of luminal lysosomal hydrolases.

Our finding that palmitoylation is required for the trafficking of Syt VII out of the TGN points to the Golgi complex as the likely site where association with CD63 occurs. This conclusion is in agreement with the increasingly prevalent view that the Golgi apparatus is a palmitoylation "hot spot." Of the 23 known human palmitoyl transferases, 12 localize to the Golgi (Fernández-Hernando et al., 2006; Ohno et al., 2006; for review see Charollais and Van Der Goot, 2009). Accumulation of the Syt VII palmitoylation–defective mutant in the Golgi is consistent with earlier studies of the retention of membrane proteins lacking palmitoylation in the Golgi complex, such as the linker for activation of T cells protein (Tanimura et al., 2006) and the Gα heterotrimeric G protein subunit (Michaelson et al., 2002). Importantly, wild-type Syt VII also failed to exit the TGN when cells were depleted in CD63, demonstrating that other tetraspanin proteins that traffic through the Golgi cannot compensate for the absence of CD63. This finding suggests the existence of a mechanism to ensure the specific association of Syt VII with CD63, as both proteins traffic through the secretory pathway. One possibility is that this is achieved through the colocalization of Syt VII and CD63 with a specific palmitoyl transferase at a particular site within the Golgi complex. In agreement with this view, in neuronal cells, the Golgi palmitoyl acyltransferase HIP14 is known to promote palmitoylation of Syt I, but not Syt VII (Huang et al., 2004). Expression of HIP14 enhances palmitoylation of a subset of synaptic proteins in addition to Syt I, reinforcing the view that palmitoylation regulates plasma membrane reorganization and formation of signaling scaffolds in neurons (Gauthier-Campbell et al., 2004; Huang et al., 2004). Our present results suggest that TEMs enriched in palmitoylated CD63 and Syt VII may play a similar role in several cell types.

Despite its steady-state late endosomal/lysosomal localization in most cells, CD63 also transits through the plasma membrane (Pols and Klumperman, 2009). Thus, by exiting the Golgi as a complex with CD63, Syt VII may also follow this tetraspanin when it traffics to the plasma membrane. Whether CD63 and Syt VII are reinternalized together is likely to depend on the stability of the palmitoylation modifications upon arrival at the plasma membrane. Very little is currently known about palmitoyl protein thioesterases, the enzymes responsible for reversing palmitoylation, and their subcellular localization, but this issue may soon become amenable to investigation (for review see Charollais and Van Der Goot, 2009). It was reported that the reinternalization of Syt VII from the plasma membrane is regulated by at least two distinct internalization signals and one inhibitory motif located in the C2 domains (Dasgupta and Kelly, 2003), implying that retrieval of this Ca^{2+} sensor may be subject to complex regulation, perhaps involved in coupling exocytosis and compensatory endocytosis (Dasgupta and Kelly, 2003).

Most members of the tetraspanin family, including CD63, are also palmitoylated in the Golgi complex (Yang et al., 2002). Palmitoylation is thought to play a central role in the ability of tetraspanins to organize themselves and other palmitoylated molecules into dynamic signaling microdomains called TEMs (Yang et al., 2004; Israels and McMillan-Ward, 2010). Our ability to coimmunoprecipitate CD63 and Syt VII, but not palmitoylation-defective Syt VII, under the mild detergent extraction conditions known to preserve TEMs (Yang et al., 2004) is consistent with the possibility that Syt VII and CD63 assemble into such dynamic membrane scaffolds (Fig. 7). The presence of Syt VII within CD63-containing TEMs that can be translocated to the cell surface in response to Ca^{2+} raises the intriguing possibility that additional components of the exocytic machinery may also be recruited to these microdomains through palmitoylation. In agreement with this possibility, the Ca^{2+} sensor

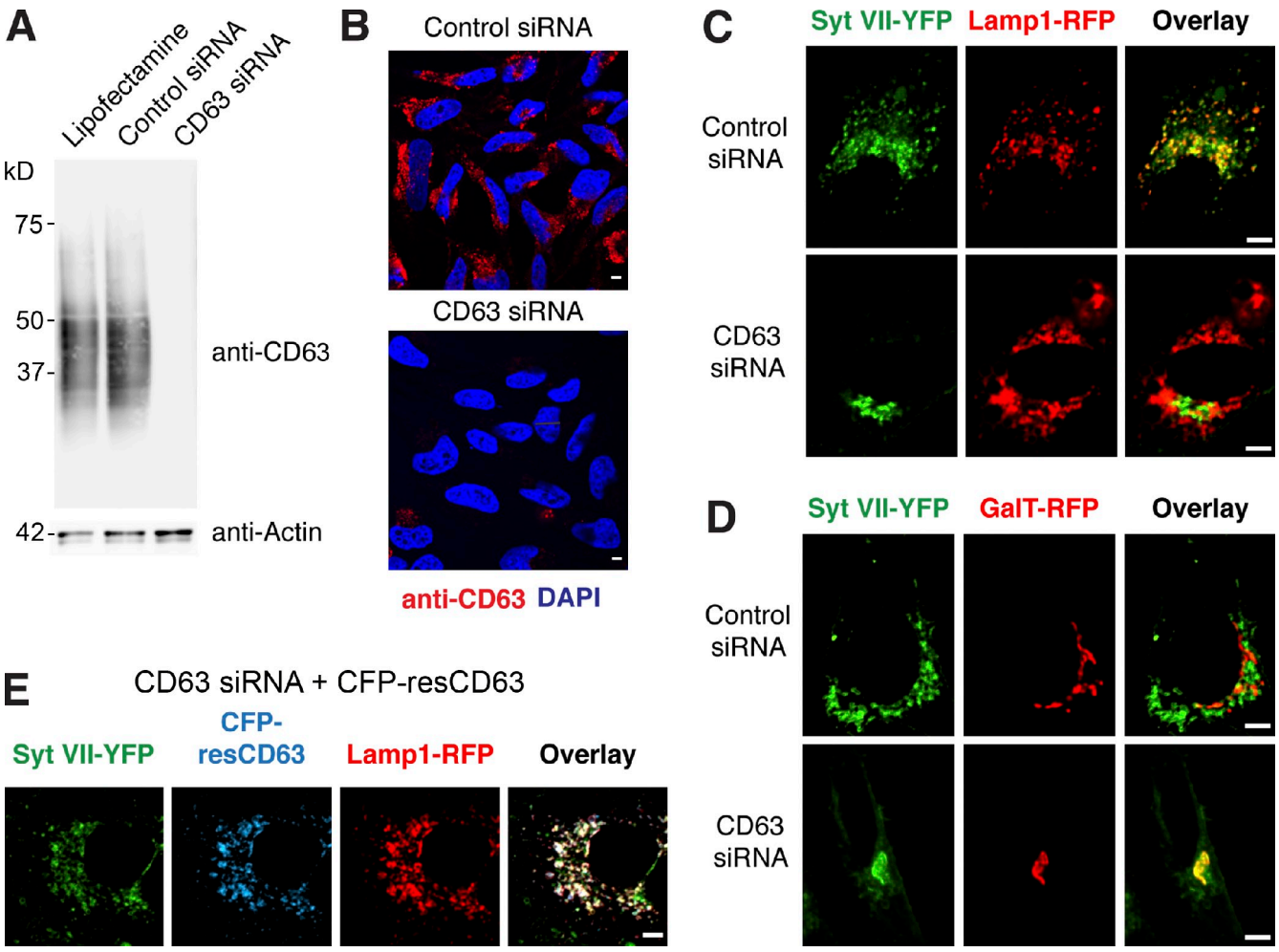

Figure 9. **CD63 is required for Syt VII trafficking to lysosomes.** (A) HeLa cells were treated with Lipofectamine alone, control siRNA, or CD63 siRNA. Immunoblotting was performed with anti-CD63 antibodies. Antiactin antibodies were used as loading controls. (B) Fluorescence confocal images of cells treated with control or CD63 siRNA after fixation, permeabilization, immunofluorescence with antibodies to CD63, and DNA staining with DAPI. (C and D) HeLa cells treated with control or CD63 siRNA were transduced with adenovirus expressing Syt VII–YFP and Lamp1-RFP or GalT-RFP and imaged by live confocal microscopy. CD63 transcriptional silencing abolished the colocalization of Syt VII–YFP with Lamp1-RFP (C), causing its retention in the Golgi (D). (E) HeLa cells treated with control or CD63 siRNA were transduced with adenovirus expressing Syt VII–YFP, Lamp1-RFP, and CFP-resCD63, encoding silent mutations rendering the transcript resistant to CD63 siRNA-mediated silencing. CFP-resCD63 expression was not inhibited by CD63 siRNA, allowing normal colocalization of Syt VII–YFP with Lamp1-RFP. Bars, 6 µm.

Syt I and the SNARE molecules syntaxin 1, SNAP25, and VAMP2 are palmitoylated in neurons (Prescott et al., 2009). Interestingly, the cysteines that serve as palmitoylation sites in Syt I are also required for its oligomerization (Fukuda et al., 2001b), suggesting that the self-association properties reported for Syt VII (Fukuda and Mikoshiba, 2000) might be related to their ability to assembly into TEMs.

The lysosomal membrane proteins Lamp1 and Lamp2 are predominantly located on the limiting membrane of lysosomal organelles, whereas CD63 and other tetraspanins are enriched in intraluminal vesicles (Escola et al., 1998; Trajkovic et al., 2008). There is also evidence for partitioning between Lamp1 and Syt VII localization within lysosomal membranes, particularly within the extensive tubular compartments of primary macrophages (Czibener et al., 2006). In this study, we show that Syt VII and CD63 move rapidly and simultaneously from lysosomes to nascent phagosomes before the delivery of Lamp1. Such differences in dynamic behavior between CD63 and Lamp1 were also seen in experiments on phagosomes containing *Cryptococcus neoformans*, which required acidification for the recruitment of CD63, but not of Lamp1 (Artavanis-Tsakonas et al., 2006). These observations reinforce our hypothesis that Syt VII and CD63 coassemble into unique, dynamic lysosomal TEMs that can be rapidly translocated to the plasma membrane upon Ca^{2+} stimulation. The palmitoylation-dependent complexes containing Syt VII and CD63 that we identify in this study should now facilitate further characterization of the molecular machinery responsible for the mobilization and fusion of lysosomal compartments with the plasma membrane.

Materials and methods

Cell culture

Mouse BMMs were prepared from C57BL/6 Syt VII$^{-/-}$ mice (Chakrabarti et al., 2003) as previously described (Roy et al., 2004). Macrophages were seeded on 24-well plates (0.5 ml of a 1.5 × 10^5–BMM/ml suspension) for phagocytosis assays or 35-mm glass-bottom dishes (2.0 ml of a

0.5×10^5–BMM/ml suspension; MatTek Corporation) 24 h before experiments and incubated in BMM-imaging media (RPMI without phenol red, 10% FBS, 20% L cell–conditioned supernatant, and 1% penicillin/streptomycin) at 37°C and 5% CO_2.

NRK cells were seeded on 35-mm glass-bottom dishes (2.0 ml of a 0.5×10^5–cell/ml suspension) 24 h before experiments in DME (10% FBS, 1% penicillin/streptomycin, and 1 mM sodium pyruvate) and incubated at 37°C and 5% CO_2. HeLa CCL-2 cells (American Type Culture Collection) were seeded on 35-mm glass-bottom dishes (2.0 ml of 0.75×10^5 cells/ml) 24 h before experiments in DME (10% FBS and 1% penicillin/streptomycin) and incubated at 37°C and 5% CO_2.

Site-directed mutagenesis, adenoviral vector construction, and adenoviral amplification

The C35S, C38S, and C41S mutations that result in a palmitoylation-deficient Syt VII protein were introduced into the Syt VII–YFP plasmid pLZRS–Syt VII–YFP (Czibener et al., 2006) using a site-directed mutagenesis kit (QuikChange; Agilent Technologies) to yield the pLZRS–Syt VII (C/S)–YFP plasmid. The Syt VII–YFP, Syt VII (C/S)–YFP, and Syt VII (D/N)–YFP constructs (Czibener et al., 2006) were cloned into NotI and EcoRV sites of the pShuttle-cytomegalovirus (CMV) plasmid (Agilent Technologies) to yield pSCMV–Syt VII–YFP, pSCMV–Syt VII (C/S)–YFP, and pSCMV–Syt VII (D/N)–YFP. Plasmids encoding the Syt VII single- and double-cysteine mutants were generated via site-directed mutagenesis using the pSCMV–Syt VII–YFP plasmid as the template to yield the constructs pSCMV–Syt VII (C35S)–YFP, pSCMV–Syt VII (C38S)–YFP, pSCMV–Syt VII (C41S)–YFP, pSCMV–Syt VII (C35/38S)–YFP, pSCMV–Syt VII (C35/41S)–YFP, and pSCMV–Syt VII (C38/41S)–YFP.

For CFP-CD63, restriction fragments were generated for the CFP-tagged human CD63 (NotI–EcoRV) from the pLZRS-CFP-CD63 plasmid (Czibener et al., 2006) and for RFP-tagged rat Lamp1 (HindIII–EcoRV) from the pLZRS-Lamp1-RFP plasmid (Czibener et al., 2006) by PCR using primers encoding the aforementioned sites. The restriction fragments were cloned into pShuttle-CMV using the same sites to yield pSCMV-CFP-CD63 and pSCMV-Lamp1-RFP. A plasmid encoding an RNAi-resistant CFP-CD63, pSCMV-CFP-resCD63, was constructed by creating silent mutations in the coding sequence target of the siRNA (5′-GGGGCCTGCAAGGAGAAC-TATTGTCTT-3′ to 5′-GGAGCTTGTAAAGAGAATTACTGCCTC-3′) by inverse PCR using pSCMV-CFP-CD63 as a template. The Y261A mutation in CD63 that blocks its lysosomal localization was introduced by a site-directed mutagenesis kit (QuikChange) into the plasmid pLZRS-CFP-CD63, followed by cloning into the NotI and EcoRV sites of pShuttle-CMV to yield pSCMV-CFP-CD63-Y/A. A restriction fragment (SnaBI–NotI) containing GalT-RFP was generated directly from pgalT-RFP (a gift from B. Lindenbach, Yale University, New Haven, CT; Murata et al., 2006) and cloned into the same restriction sites of pShuttle-CMV to yield pSCMV-GalT-RFP.

The plasmid encoding a 3×FLAG epitope–tagged CD63 was generated by first amplifying the CD63 ORF from plasmid pLZRS-CFP-CD63 with primers encoding an NruI site immediately after the start codon of CD63 to yield a fragment flanked by NotI and EcorV restriction sites. The resulting fragment was then cloned into the pCR4Blunt-TOPO vector using the Zero Blunt TOPO PCR Cloning kit (Invitrogen) to generate the pTopo-NruI-CD63 plasmid. A blunt-end DNA fragment encoding the 3×FLAG epitope tag (Sigma-Aldrich) was amplified and cloned into the NruI site of pTopo-NruI-CD63. The resulting ORF encoding 3×FLAG-CD63 was cloned into the NotI and EcoRV sites of pShuttle-CMV to yield pSCMV-3×FLAG-CD63. The Y261A mutation in CD63 that blocks its lysosomal localization was introduced by a site-directed mutagenesis kit (QuikChange) into the plasmid pLZRS-CFP-CD63, followed by cloning into the NotI and EcoRV sites of pShuttle-CMV to yield pSCMV-CFP-CD63-Y/A. To generate a plasmid encoding the 3×FLAG-CD63 Y261A mutant, a site-directed mutagenesis kit (QuikChange) was used with pSCMV-3×FLAG-CD63 to yield pSCMV-3×FLAG-CD63-Y/A.

The resulting pShuttle-CMV vectors were transformed into BJ5183-AD-1 cells (Agilent Technologies) and screened for pAdEasy-1 recombinants as outlined in the AdEasy XL Adenoviral Vector System manual (Agilent Technologies). Adenovirus production and amplification were performed as previously described (Luo et al., 2007). Virus purification and concentration were accomplished using an adenovirus purification column (Virakit; Virapur) according to the manufacturer's protocol. The purified virus was titered by plaque assay and frozen at −80°C.

Adenoviral transduction, live-cell imaging, and image analysis

Before live-cell imaging experiments, BMMs or NRK cells were seeded in glass-bottom dishes and allowed to attach for 6 h in BMM or NRK media at 37°C and 5% CO_2. For Syt VII$^{-/-}$ BMMs, the cells were transduced for 18 h by replacing the culture media with BMM-imaging media containing purified adenovirus encoding Syt VII–YFP or Syt VII (C/S)–YFP and Lamp1-RFP at a 100:1 MOI for each strain of adenovirus. For NRKs, cells were transduced for 18 h by replacing the culture media with NRK-imaging media (DME without phenol red [10% FBS, 1% penicillin/streptomycin, and 1 mM sodium pyruvate]) containing purified adenovirus encoding Syt VII–YFP or Syt VII (C/S)–YFP in addition to adenovirus encoding either Lamp1-RFP or GalT-RFP at a 50:1 MOI. For HeLa, cells were transduced for 18 h by replacing the culture media with HeLa-imaging media (DME without phenol red [10% FBS and 1% penicillin/streptomycin]) containing purified adenovirus encoding Syt VII–YFP in addition to adenovirus encoding either Lamp1-RFP or GalT-RFP at a 10:1 MOI. For the siRNA rescue experiments, HeLa cells were also transduced with adenovirus encoding CFP-resCD63 at a 10:1 MOI.

For imaging, dishes were placed in a chamber (LiveCell System; Pathology Devices, Inc.) at 37°C with 5% CO_2 attached to an inverted microscope with a 60× NA 1.4 objective (Eclipse Ti; Nikon). Spinning-disk confocal images were acquired using the UltraVIEW VoX system (PerkinElmer) equipped with a camera (C9100-50; Hamamatsu), analyzed, and edited using the Volocity Software Suite (PerkinElmer). Final image γ settings were changed to 1.4.

Phagocytosis assays

Microscopy-based phagocytosis assays were conducted as previously reported (Czibener et al., 2006). In brief, Syt VII$^{-/-}$ BMMs were transduced with adenovirus encoding Syt VII–YFP, Syt VII (C/S)–YFP, or Syt VII (D/N)–YFP at an MOI of 100:1 for 24 h. After transduction, zymosan red bioparticles (Invitrogen) were incubated for 1 h at a ratio of 25 particles per cell. The cells were washed four times with PBS and fixed for 15 min in 4% PFA. Coverslips were mounted with antifade reagent (ProLong Gold; Invitrogen) and analyzed on a microscope (Axiovert 200; Carl Zeiss, Inc.) equipped with a camera (CoolSNAP HQ; Roper Industries) controlled by Metamorph software (MDS Analytical Technologies). The number of zymosan particles within 300–350 BMMs was determined microscopically for each construct. For live-cell imaging of zymosan uptake, BMMs were transduced with adenovirus encoding Syt VII–YFP or Syt VII (C/S)–YFP in addition to Lamp1-RFP and CFP-CD63 as described in the previous section. After 24 h, unlabeled zymosan particles were added to the glass-bottom dishes at a ratio of 10 particles per cell, and images were acquired at one frame every 10 s on the spinning-disk confocal microscope system as described in the previous section. All videos were analyzed and edited using the Volocity software suite and exported as video files (QuickTime; Apple).

CD63 transcriptional silencing and complementation with ectopically expressed CD63

HeLa cells were transfected with Lipofectamine RNAiMAX (Invitrogen) and 160 pmol of medium G-C content control (12935300) or CD63 (HSS101615; [RNA] 5′-GGCCUGCAAGGAGAACUAUUGUCUU-3′) Stealth siRNA duplexes according to the manufacturer's instructions (Invitrogen). At 24 h after transfection, the cells were transfected again as outlined in the previous section. At 48 h after the initial transfection, the cells were transduced with adenovirus expressing Syt VII–YFP, Lamp1-RFP, GalT-RFP, and/or CFP-resCD63 and imaged as outlined in the previous section.

Palmitoylation inhibition, live-cell imaging, and image analysis

NRK cells were seeded in glass-bottom dishes and allowed to attach to the dish for 6 h. The NRK media were then replaced with DME without phenol red containing 2.5% FBS, 0.25% defatted BSA (Sigma-Aldrich), 1 mM sodium pyruvate, and 1% penicillin/streptomycin with or without 2-BP (Sigma-Aldrich) as previously described (Webb et al., 2000). The cells were simultaneously transduced with adenovirus encoding Lamp1-RFP or GalT-RFP and either Syt VII–YFP or Syt VII (C/S)–YFP for 15 h and imaged as described in the previous section.

For washout experiments, the 2-BP media were replaced with NRK-imaging media, and the glass-bottom dishes were placed in the LiveCell System chamber. Cells were imaged with the spinning-disk confocal microscopy system as described in the previous section at one focal plane maintained by the Perfect Focus System (Nikon), capturing one image every minute. All videos were analyzed and edited using the Volocity software suite and exported as QuickTime video files.

Immunofluorescence and confocal imaging

HeLa cells treated with siRNA as described in the previous section were washed with PBS, fixed with 5% PFA, washed and incubated with 50 mM NH_4Cl_2 for 30 min, and permeabilized with 0.1% saponin and 1.0% BSA in PBS. Permeabilized cells were incubated with blocking buffer (5.0% horse serum, 1.0% BSA, and 0.1% saponin in PBS) for 1 h,

washed, and incubated with mouse anti-CD63 (H5C6; Developmental Studies Hybridoma Bank) for 1 h, followed by Alexa Fluor 594–conjugated goat anti–mouse antibodies (Invitrogen) for 1 h and DAPI staining before imaging on a confocal microscope (TCS SP5 X Supercontinuum Confocal; Leica) using a 63× NA 1.2 objective. Image acquisition was performed with the application suite software package (Leica). Image analysis was performed with the Volocity software suite. Final image γ settings were changed to 1.4.

Immunoprecipitations and Western blot analysis

To generate whole-cell lysates, Syt VII$^{-/-}$ BMMs transduced with Syt VII–YFP, Syt VII (D/N)–YFP, or Syt VII (C/S)–YFP for 24 h or HeLa cells treated with siRNA as described in the previous section were lysed in whole-cell lysate buffer (25 mM Hepes, pH 7.4, 150 mM NaCl, 1% Triton X-100, and Complete Protease Inhibitor Cocktail [Roche]) at 4°C for 1 h. Lysates were clarified by centrifugation at 10,000 *g* for 10 min, and the total amount of protein was determined by bicinchoninic acid (Thermo Fisher Scientific). A volume of clarified lysate containing 20 µg of protein was added to 6× SDS sample buffer, resolved on 10% SDS-PAGE, transferred to nitrocellulose, and probed with either rabbit anti-GFP antibodies (1:1,000; Invitrogen), mouse anti-CD63 antibodies (H5C6, 1:200), or mouse anti–β-actin (1:1,000; Sigma-Aldrich). Blots were then incubated with either peroxidase-conjugated donkey anti–rabbit or donkey anti–mouse antibodies (1:10,000; Jackson ImmunoResearch Laboratories, Inc.), washed, incubated for 5 min with HRP solution (Immun-Star; Bio-Rad Laboratories), and visualized on an imaging system (LAS-3000; Fujifilm). Relative protein levels were determined using the ImageJ software (National Institutes of Health).

FLAG-CD63 coimmunoprecipitations were performed as previously described (Duffield et al., 2003). In brief, NRK cells were seeded in 6-well tissue-culture dishes (2 ml of 2.5 × 10^5 cells/ml) and allowed to attach to the dish for 6 h. The cells were transduced with adenovirus encoding Syt VII–YFP, Syt VII–YFP/FLAG-CD63, Syt VII (C/S)–YFP/FLAG-CD63, Syt VII–YFP/FLAG-CD63 (Y/A), or Syt VII (C/S)–YFP/FLAG-CD63 (Y/A) and incubated at 37°C and 5% CO_2 for 15 h. The cells were then washed with PBS, trypsinized, and resuspended at 1.0 × 10^6 cells/ml. The 1-ml cell suspensions were incubated in lysis buffer (5 mM $MgCl_2$, 150 mM NaCl, 25 mM Hepes, pH 7.4, and Complete Protease Inhibitor Cocktail) supplemented with 1% Brij-97 (Sigma-Aldrich) at 4°C for 1 h. The lysates were cleared by centrifugation at 10,000 *g* for 30 min at 4°C and incubated with a 20-µl bed volume of anti-FLAG M2 affinity gel (EZview red; Sigma-Aldrich) for 2 h at 4°C. The affinity gel was collected by centrifugation and washed four times in 1% Brij-97 lysis buffer at 4°C. After the final wash, the resin and samples of the clarified lysates were treated with PNGase F (New England Biolabs, Inc.) as directed by the manufacturer. Clarified lysates were then precipitated on ice with 25% TCA, washed with ice-cold acetone, and resuspended in SDS-PAGE sample buffer containing 5% β-mercaptoethanol. The PNGase F–treated resin was incubated in SDS-PAGE sample buffer containing 5% β-mercaptoethanol and heated to 65°C for 10 min. The samples were resolved on SDS–10% PAGE and transferred to nitrocellulose membranes. To monitor loading levels, membranes were stained with Ponceau S stain (Sigma-Aldrich). After blocking with 5% dry milk, membranes were incubated for 2 h with mouse anti-FLAG-peroxidase (HRP) antibody (1:1,000; Sigma-Aldrich), rabbit anti-GFP antibody (1:1,000; Invitrogen), or mouse antiactin (1:1,000; Sigma-Aldrich) at room temperature followed by peroxidase-conjugated antibodies and visualization as described in the previous section.

Online supplemental material

Fig. S1 shows a live-cell confocal image demonstrating that Syt VII (C/S)–YFP colocalizes with the Golgi marker GalT-RFP in bone marrow–derived macrophages. Video 1 shows the simultaneous recruitment of Syt VII–YFP and CFP-CD63 to nascent phagosomes, followed by Lamp1-RFP recruitment from dynamic tubular compartments surrounding the recently formed phagosome. Video 2 shows CFP-CD63, but not Syt VII (C/S)–YFP recruitment to nascent phagosomes. Lamp1 is detected in the phagosome, but only at later time points. Video 3 shows the redistribution of Syt VII–YFP to Lamp1-RFP–positive vesicles upon washout of the palmitoylation inhibitor 2-BP. Video 4 shows a stack of 16 confocal Z sections at intervals of 0.2 µm from an NRK cell expressing Syt VII–YFP, Lamp1-RFP, and either CFP-CD63 or CFP-CD63 (Y/A). Video 5 shows a stack of 16 confocal Z sections at intervals of 0.2 µm from an NRK cell expressing Syt VII (C/S)–YFP, Lamp1-RFP, and either CFP-CD63 or CFP-CD63 (Y/A). Online supplemental material is available at http://www.jcb.org/cgi/content/full/jcb.201003021/DC1.

We would like to thank Dr. Brett Lindenbach for providing the pgalT-RFP plasmid and Amy Beaven and the Cell Biology and Molecular Genetics Imaging Core for assistance with confocal microscopy.

This work was supported by National Institutes of Health grant F32 GM082145 to A.R. Flannery and National Institutes of Health grant RO1 GM064625 to N.W. Andrews.

Submitted: 05 March 2010
Accepted: 05 October 2010

References

Abrami, L., S.H. Leppla, and F.G. van der Goot. 2006. Receptor palmitoylation and ubiquitination regulate anthrax toxin endocytosis. *J. Cell Biol.* 172:309–320. doi:10.1083/jcb.200507067

Andrews, N.W., and S. Chakrabarti. 2005. There's more to life than neurotransmission: the regulation of exocytosis by synaptotagmin VII. *Trends Cell Biol.* 15:626–631. doi:10.1016/j.tcb.2005.09.001

Artavanis-Tsakonas, K., J.C. Love, H.L. Ploegh, and J.M. Vyas. 2006. Recruitment of CD63 to *Cryptococcus neoformans* phagosomes requires acidification. *Proc. Natl. Acad. Sci. USA.* 103:15945–15950. doi:10.1073/pnas.0607528103

Becker, S.M., L. Delamarre, I. Mellman, and N.W. Andrews. 2009. Differential role of the Ca(2+) sensor synaptotagmin VII in macrophages and dendritic cells. *Immunobiology.* 214:495–505. doi:10.1016/j.imbio.2008.11.006

Bhalla, A., W.C. Tucker, and E.R. Chapman. 2005. Synaptotagmin isoforms couple distinct ranges of Ca2+, Ba2+, and Sr2+ concentration to SNARE-mediated membrane fusion. *Mol. Biol. Cell.* 16:4755–4764. doi:10.1091/mbc.E05-04-0277

Blagoveshchenskaya, A.D., E.W. Hewitt, and D.F. Cutler. 1999. Di-leucine signals mediate targeting of tyrosinase and synaptotagmin to synaptic-like microvesicles within PC12 cells. *Mol. Biol. Cell.* 10:3979–3990.

Bonifacino, J.S., and L.M. Traub. 2003. Signals for sorting of transmembrane proteins to endosomes and lysosomes. *Annu. Rev. Biochem.* 72:395–447. doi:10.1146/annurev.biochem.72.121801.161800

Braulke, T., and J.S. Bonifacino. 2009. Sorting of lysosomal proteins. *Biochim. Biophys. Acta.* 1793:605–614. doi:10.1016/j.bbamcr.2008.10.016

Braun, V., V. Fraisier, G. Raposo, I. Hurbain, J.-B. Sibarita, P. Chavrier, T. Galli, and F. Niedergang. 2004. TI-VAMP/VAMP7 is required for optimal phagocytosis of opsonised particles in macrophages. *EMBO J.* 23:4166–4176. doi:10.1038/sj.emboj.7600427

Caler, E.V., S. Chakrabarti, K.T. Fowler, S. Rao, and N.W. Andrews. 2001. The exocytosis-regulatory protein synaptotagmin VII mediates cell invasion by *Trypanosoma cruzi*. *J. Exp. Med.* 193:1097–1104. doi:10.1084/jem.193.9.1097

Chakrabarti, S., K.S. Kobayashi, R.A. Flavell, C.B. Marks, K. Miyake, D.R. Liston, K.T. Fowler, F.S. Gorelick, and N.W. Andrews. 2003. Impaired membrane resealing and autoimmune myositis in synaptotagmin VII–deficient mice. *J. Cell Biol.* 162:543–549. doi:10.1083/jcb.200305131

Chapman, E.R. 2008. How does synaptotagmin trigger neurotransmitter release? *Annu. Rev. Biochem.* 77:615–641. doi:10.1146/annurev.biochem.77.062005.101135

Charollais, J., and F.G. Van Der Goot. 2009. Palmitoylation of membrane proteins (Review). *Mol. Membr. Biol.* 26:55–66. doi:10.1080/09687680802620369

Codina, J., J. Li, and T.D. Dubose Jr. 2005. CD63 interacts with the carboxy terminus of the colonic H+-K+-ATPase to decrease [corrected] plasma membrane localization and 86Rb+ uptake. *Am. J. Physiol. Cell Physiol.* 288:C1279–C1286. doi:10.1152/ajpcell.00463.2004

Czibener, C., N.M. Sherer, S.M. Becker, M. Pypaert, E. Hui, E.R. Chapman, W. Mothes, and N.W. Andrews. 2006. Ca^{2+} and synaptotagmin VII–dependent delivery of lysosomal membrane to nascent phagosomes. *J. Cell Biol.* 174:997–1007. doi:10.1083/jcb.200605004

Dasgupta, S., and R.B. Kelly. 2003. Internalization signals in synaptotagmin VII utilizing two independent pathways are masked by intramolecular inhibitions. *J. Cell Sci.* 116:1327–1337. doi:10.1242/jcs.00290

Duffield, A., E.J. Kamsteeg, A.N. Brown, P. Pagel, and M.J. Caplan. 2003. The tetraspanin CD63 enhances the internalization of the H,K-ATPase beta-subunit. *Proc. Natl. Acad. Sci. USA.* 100:15560–15565. doi:10.1073/pnas.2536699100

Escola, J.M., M.J. Kleijmeer, W. Stoorvogel, J.M. Griffith, O. Yoshie, and H.J. Geuze. 1998. Selective enrichment of tetraspan proteins on the internal vesicles of multivesicular endosomes and on exosomes secreted by human B-lymphocytes. *J. Biol. Chem.* 273:20121–20127. doi:10.1074/jbc.273.32.20121

Fernández-Hernando, C., M. Fukata, P.N. Bernatchez, Y. Fukata, M.I. Lin, D.S. Bredt, and W.C. Sessa. 2006. Identification of Golgi-localized acyl

transferases that palmitoylate and regulate endothelial nitric oxide synthase. *J. Cell Biol.* 174:369–377. doi:10.1083/jcb.200601051

Fukuda, M. 2002. Vesicle-associated membrane protein-2/synaptobrevin binding to synaptotagmin I promotes O-glycosylation of synaptotagmin I. *J. Biol. Chem.* 277:30351–30358. doi:10.1074/jbc.M204056200

Fukuda, M., and K. Mikoshiba. 2000. Distinct self-oligomerization activities of synaptotagmin family. Unique calcium-dependent oligomerization properties of synaptotagmin VII. *J. Biol. Chem.* 275:28180–28185.

Fukuda, M., K. Ibata, and K. Mikoshiba. 2001a. A unique spacer domain of synaptotagmin IV is essential for Golgi localization. *J. Neurochem.* 77:730–740. doi:10.1046/j.1471-4159.2001.00266.x

Fukuda, M., E. Kanno, Y. Ogata, and K. Mikoshiba. 2001b. Mechanism of the SDS-resistant synaptotagmin clustering mediated by the cysteine cluster at the interface between the transmembrane and spacer domains. *J. Biol. Chem.* 276:40319–40325.

Fukuda, M., E. Kanno, M. Satoh, C. Saegusa, and A. Yamamoto. 2004. Synaptotagmin VII is targeted to dense-core vesicles and regulates their Ca2+-dependent exocytosis in PC12 cells. *J. Biol. Chem.* 279:52677–52684. doi:10.1074/jbc.M409241200

Gao, Z., J. Reavey-Cantwell, R.A. Young, P. Jegier, and B.A. Wolf. 2000. Synaptotagmin III/VII isoforms mediate Ca2+-induced insulin secretion in pancreatic islet beta-cells. *J. Biol. Chem.* 275:36079–36085. doi:10.1074/jbc.M004284200

Gauthier, B.R., D.L. Duhamel, M. Iezzi, S. Theander, F. Saltel, M. Fukuda, B. Wehrle-Haller, and C.B. Wollheim. 2008. Synaptotagmin VII splice variants alpha, beta, and delta are expressed in pancreatic beta-cells and regulate insulin exocytosis. *FASEB J.* 22:194–206. doi:10.1096/fj.07-8333com

Gauthier-Campbell, C., D.S. Bredt, T.H. Murphy, and Ael.-D. El-Husseini. 2004. Regulation of dendritic branching and filopodia formation in hippocampal neurons by specific acylated protein motifs. *Mol. Biol. Cell.* 15:2205–2217. doi:10.1091/mbc.E03-07-0493

Geppert, M., B.T. Archer III, and T.C. Südhof. 1991. Synaptotagmin II. A novel differentially distributed form of synaptotagmin. *J. Biol. Chem.* 266:13548–13552.

Gustavsson, N., Y. Lao, A. Maximov, J.C. Chuang, E. Kostromina, J.J. Repa, C. Li, G.K. Radda, T.C. Südhof, and W. Han. 2008. Impaired insulin secretion and glucose intolerance in synaptotagmin-7 null mutant mice. *Proc. Natl. Acad. Sci. USA.* 105:3992–3997. doi:10.1073/pnas.0711700105

Gustavsson, N., S.H. Wei, D.N. Hoang, Y. Lao, Q. Zhang, G.K. Radda, P. Rorsman, T.C. Südhof, and W. Han. 2009. Synaptotagmin-7 is a principal Ca2+ sensor for Ca2+-induced glucagon exocytosis in pancreas. *J. Physiol.* 587:1169–1178. doi:10.1113/jphysiol.2008.168005

Haberman, Y., I. Ziv, Y. Gorzalczany, M. Fukuda, and R. Sagi-Eisenberg. 2005. Classical protein kinase C(s) regulates targeting of synaptotagmin IX to the endocytic recycling compartment. *J. Cell Sci.* 118:1641–1649. doi:10.1242/jcs.02276

Han, W., J.S. Rhee, A. Maximov, Y. Lao, T. Mashimo, C. Rosenmund, and T.C. Südhof. 2004. N-glycosylation is essential for vesicular targeting of synaptotagmin 1. *Neuron.* 41:85–99. doi:10.1016/S0896-6273(03)00820-1

Heindel, U., M.F. Schmidt, and M. Veit. 2003. Palmitoylation sites and processing of synaptotagmin I, the putative calcium sensor for neurosecretion. *FEBS Lett.* 544:57–62. doi:10.1016/S0014-5793(03)00449-6

Huang, K., A. Yanai, R. Kang, P. Arstikaitis, R.R. Singaraja, M. Metzler, A. Mullard, B. Haigh, C. Gauthier-Campbell, C.A. Gutekunst, et al. 2004. Huntingtin-interacting protein HIP14 is a palmitoyl transferase involved in palmitoylation and trafficking of multiple neuronal proteins. *Neuron.* 44:977–986. doi:10.1016/j.neuron.2004.11.027

Idone, V., C. Tam, and N.W. Andrews. 2008. Two-way traffic on the road to plasma membrane repair. *Trends Cell Biol.* 18:552–559. doi:10.1016/j.tcb.2008.09.001

Iezzi, M., G. Kouri, M. Fukuda, and C.B. Wollheim. 2004. Synaptotagmin V and IX isoforms control Ca2+-dependent insulin exocytosis. *J. Cell Sci.* 117:3119–3127. doi:10.1242/jcs.01179

Israels, S.J., and E.M. McMillan-Ward. 2010. Palmitoylation supports the association of tetraspanin CD63 with CD9 and integrin alphaIIb-beta3 in activated platelets. *Thromb. Res.* 125:152–158. doi:10.1016/j.thromres.2009.07.005

Jaiswal, J.K., N.W. Andrews, and S.M. Simon. 2002. Membrane proximal lysosomes are the major vesicles responsible for calcium-dependent exocytosis in non-secretory cells. *J. Cell Biol.* 159:625–635. doi:10.1083/jcb.200208154

Kabayama, H., K. Takei, M. Fukuda, K. Ibata, and K. Mikoshiba. 1999. Functional involvement of synaptotagmin I/II C2A domain in neurite outgrowth of chick dorsal root ganglion neuron. *Neuroscience.* 88:999–1003. doi:10.1016/S0306-4522(98)00547-8

Källquist, L., M. Hansson, A.M. Persson, H. Janssen, J. Calafat, H. Tapper, and I. Olsson. 2008. The tetraspanin CD63 is involved in granule targeting of neutrophil elastase. *Blood.* 112:3444–3454. doi:10.1182/blood-2007-10-116285

Kang, R., R. Swayze, M.F. Lise, K. Gerrow, A. Mullard, W.G. Honer, and A. El-Husseini. 2004. Presynaptic trafficking of synaptotagmin I is regulated by protein palmitoylation. *J. Biol. Chem.* 279:50524–50536. doi:10.1074/jbc.M404981200

Kanno, E., and M. Fukuda. 2008. Increased plasma membrane localization of O-glycosylation-deficient mutant of synaptotagmin I in PC12 cells. *J. Neurosci. Res.* 86:1036–1043. doi:10.1002/jnr.21568

Keefe, D., L. Shi, S. Feske, R. Massol, F. Navarro, T. Kirchhausen, and J. Lieberman. 2005. Perforin triggers a plasma membrane-repair response that facilitates CTL induction of apoptosis. *Immunity.* 23:249–262. doi:10.1016/j.immuni.2005.08.001

Krasnov, P.A., and G. Enikolopov. 2000. Targeting of synaptotagmin to neurite terminals in neuronally differentiated PC12 cells. *J. Cell Sci.* 113:1389–1404.

Li, C., B. Ullrich, J.Z. Zhang, R.G. Anderson, N. Brose, and T.C. Südhof. 1995. Ca(2+)-dependent and -independent activities of neural and non-neural synaptotagmins. *Nature.* 375:594–599. doi:10.1038/375594a0

Li, Y., P. Wang, J. Xu, F. Gorelick, H. Yamazaki, N. Andrews, and G.V. Desir. 2007. Regulation of insulin secretion and GLUT4 trafficking by the calcium sensor synaptotagmin VII. *Biochem. Biophys. Res. Commun.* 362:658–664. doi:10.1016/j.bbrc.2007.08.023

Luo, J., Z.L. Deng, X. Luo, N. Tang, W.X. Song, J. Chen, K.A. Sharff, H.H. Luu, R.C. Haydon, K.W. Kinzler, et al. 2007. A protocol for rapid generation of recombinant adenoviruses using the AdEasy system. *Nat. Protoc.* 2:1236–1247. doi:10.1038/nprot.2007.135

Martinez, I., S. Chakrabarti, T. Hellevik, J. Morehead, K. Fowler, and N.W. Andrews. 2000. Synaptotagmin VII regulates Ca^{2+}-dependent exocytosis of lysosomes in fibroblasts. *J. Cell Biol.* 148:1141–1149. doi:10.1083/jcb.148.6.1141

Matthew, W.D., L. Tsavaler, and L.F. Reichardt. 1981. Identification of a synaptic vesicle-specific membrane protein with a wide distribution in neuronal and neurosecretory tissue. *J. Cell Biol.* 91:257–269. doi:10.1083/jcb.91.1.257

Michaelson, D., I. Ahearn, M. Bergo, S. Young, and M. Philips. 2002. Membrane trafficking of heterotrimeric G proteins via the endoplasmic reticulum and Golgi. *Mol. Biol. Cell.* 13:3294–3302. doi:10.1091/mbc.E02-02-0095

Monterrat, C., F. Grise, M.N. Benassy, A. Hémar, and J. Lang. 2007. The calcium-sensing protein synaptotagmin 7 is expressed on different endosomal compartments in endocrine, neuroendocrine cells or neurons but not on large dense core vesicles. *Histochem. Cell Biol.* 127:625–632. doi:10.1007/s00418-007-0271-0

Murata, T., A. Delprato, A. Ingmundson, D.K. Toomre, D.G. Lambright, and C.R. Roy. 2006. The *Legionella pneumophila* effector protein DrrA is a Rab1 guanine nucleotide-exchange factor. *Nat. Cell Biol.* 8:971–977. doi:10.1038/ncb1463

Ohno, Y., A. Kihara, T. Sano, and Y. Igarashi. 2006. Intracellular localization and tissue-specific distribution of human and yeast DHHC cysteine-rich domain-containing proteins. *Biochim. Biophys. Acta.* 1761:474–483.

Pols, M.S., and J. Klumperman. 2009. Trafficking and function of the tetraspanin CD63. *Exp. Cell Res.* 315:1584–1592. doi:10.1016/j.yexcr.2008.09.020

Prescott, G.R., O.A. Gorleku, J. Greaves, and L.H. Chamberlain. 2009. Palmitoylation of the synaptic vesicle fusion machinery. *J. Neurochem.* 110:1135–1149. doi:10.1111/j.1471-4159.2009.06205.x

Reddy, A., E.V. Caler, and N.W. Andrews. 2001. Plasma membrane repair is mediated by Ca(2+)-regulated exocytosis of lysosomes. *Cell.* 106:157–169. doi:10.1016/S0092-8674(01)00421-4

Rous, B.A., B.J. Reaves, G. Ihrke, J.A. Briggs, S.R. Gray, D.J. Stephens, G. Banting, and J.P. Luzio. 2002. Role of adaptor complex AP-3 in targeting wild-type and mutated CD63 to lysosomes. *Mol. Biol. Cell.* 13:1071–1082. doi:10.1091/mbc.01-08-0409

Roy, D., D.R. Liston, V.J. Idone, A. Di, D.J. Nelson, C. Pujol, J.B. Bliska, S. Chakrabarti, and N.W. Andrews. 2004. A process for controlling intracellular bacterial infections induced by membrane injury. *Science.* 304:1515–1518. doi:10.1126/science.1098371

Schaub, B.E., B. Berger, E.G. Berger, and J. Rohrer. 2006. Transition of galactosyltransferase 1 from trans-Golgi cisterna to the trans-Golgi network is signal mediated. *Mol. Biol. Cell.* 17:5153–5162. doi:10.1091/mbc.E06-08-0665

Skubitz, K.M., K.D. Campbell, and A.P. Skubitz. 2000. CD63 associates with CD11/CD18 in large detergent-resistant complexes after translocation to the cell surface in human neutrophils. *FEBS Lett.* 469:52–56. doi:10.1016/S0014-5793(00)01240-0

Takino, T., H. Miyamori, N. Kawaguchi, T. Uekita, M. Seiki, and H. Sato. 2003. Tetraspanin CD63 promotes targeting and lysosomal proteolysis of membrane-type 1 matrix metalloproteinase. *Biochem. Biophys. Res. Commun.* 304:160–166. doi:10.1016/S0006-291X(03)00544-8

Tanimura, N., S. Saitoh, S. Kawano, A. Kosugi, and K. Miyake. 2006. Palmitoylation of LAT contributes to its subcellular localization and stability. *Biochem. Biophys. Res. Commun.* 341:1177–1183. doi:10.1016/j.bbrc.2006.01.076

Trajkovic, K., C. Hsu, S. Chiantia, L. Rajendran, D. Wenzel, F. Wieland, P. Schwille, B. Brügger, and M. Simons. 2008. Ceramide triggers budding of exosome vesicles into multivesicular endosomes. *Science.* 319:1244–1247. doi:10.1126/science.1153124

Webb, Y., L. Hermida-Matsumoto, and M.D. Resh. 2000. Inhibition of protein palmitoylation, raft localization, and T cell signaling by 2-bromopalmitate and polyunsaturated fatty acids. *J. Biol. Chem.* 275:261–270. doi:10.1074/jbc.275.1.261

Yang, X., C. Claas, S.K. Kraeft, L.B. Chen, Z. Wang, J.A. Kreidberg, and M.E. Hemler. 2002. Palmitoylation of tetraspanin proteins: modulation of CD151 lateral interactions, subcellular distribution, and integrin-dependent cell morphology. *Mol. Biol. Cell.* 13:767–781. doi:10.1091/mbc.01-05-0275

Yang, X., O.V. Kovalenko, W. Tang, C. Claas, C.S. Stipp, and M.E. Hemler. 2004. Palmitoylation supports assembly and function of integrin–tetraspanin complexes. *J. Cell Biol.* 167:1231–1240. doi:10.1083/jcb.200404100

Yoshida, T., Y. Kawano, K. Sato, Y. Ando, J. Aoki, Y. Miura, J. Komano, Y. Tanaka, and Y. Koyanagi. 2008. A CD63 mutant inhibits T-cell tropic human immunodeficiency virus type 1 entry by disrupting CXCR4 trafficking to the plasma membrane. *Traffic.* 9:540–558. doi:10.1111/j.1600-0854.2007.00700.x

Zhao, H., Y. Ito, J. Chappel, N.W. Andrews, S.L. Teitelbaum, and F.P. Ross. 2008. Synaptotagmin VII regulates bone remodeling by modulating osteoclast and osteoblast secretion. *Dev. Cell.* 14:914–925. doi:10.1016/j.devcel.2008.03.022